X-ray Photoelectron Spectroscopy of Pyridinium-Based Ionic Liquids: Comparison to Imidazolium- and Pyrrolidinium-Based Analogues

ARTICLE *in* PHYSICAL CHEMISTRY CHEMICAL PHYSICS · SEPTEMBER 2011

Impact Factor: 4.49 · DOI: 10.1039/c1cp21053j · Source: PubMed

3 AUTHORS, INCLUDING:

Peter Licence
University of Nottingham
117 PUBLICATIONS **3,675** CITATIONS

SEE PROFILE

PCCP

View Online
Dynamic Article Links

Cite this: *Phys. Chem. Chem. Phys.*, 2011, **13**, 15244–15255

www.rsc.org/pccp

PAPER

X-ray photoelectron spectroscopy of pyrrolidinium-based ionic liquids: cation–anion interactions and a comparison to imidazolium-based analogues†

Shuang Men, Kevin R. J. Lovelock*‡ and Peter Licence*

Received 5th April 2011, Accepted 23rd June 2011
DOI: 10.1039/c1cp21053j

We investigate seven 1-alkyl-1-methylpyrrolidinium-based ionic liquids, $[C_nC_1Pyrr][X]$, using X-ray photoelectron spectroscopy (XPS). The electronic environment for each element is analysed and a robust fitting model is developed for the C 1s region that applies to each of the ionic liquids studied. This model allows accurate charge correction and the determination of reliable and reproducible binding energies for each ionic liquid studied. The electronic interaction between the cation and anion is investigated for ionic liquids with one and also two anions. *i.e.*, mixtures. Comparisons are made to imidazolium-based ionic liquids; in particular, a detailed comparison is made between $[C_8C_1Pyrr][X]$ and $[C_8C_1Im][X]^-$, where X^- is common to both ionic liquids.

Introduction

Ionic liquids—low temperature molten salts composed entirely of mobile ions—are a fascinating class of materials that have experienced an incredible growth in research over recent years.[1–3] The structural diversity associated with ionic liquids is often seen as a key strength in the opportunities that may be afforded in chemical synthesis and processing. However, it is this enormous range of opportunity that can sometimes lead to unjust, and in some cases unrealistic, assumptions of trends in both physical and chemical properties. To date, the main focus of research effort, particularly in the area of surface characterisation and ultra-high vacuum (UHV) characterisation, has been upon imidazolium-based ionic liquids, quite simply because these are the materials most often employed by synthetic chemists. However, interest in pyrrolidinium-based ionic liquids has increased, particularly amongst electrochemists, due to their varied, and often superior, physicochemical properties when compared to imidazolium-based ionic liquids. Pyrrolidinium-based ionic liquids have similar melting points to their imidazolium-based analogues,[4] conductivities[5] and viscosities[6,7] are generally also slightly higher. Analysis of the long-term thermal stability of pyrrolidinium-based ionic liquids is, as with imidazolium-based ionic liquids, not yet fully understood.[8,9] Enthalpies of vaporisation at 298 K, $\Delta_{vap}H_{298}$, have been measured for four pyrrolidinium-based ionic liquids; the $\Delta_{vap}H_{298}$ values obtained are all $>$ 150 kJ mol^{-1},[10–12] which indicates that they are ultrahigh vacuum (UHV) stable at room temperature and can be investigated using UHV techniques.

X-ray photoelectron spectroscopy (XPS) is now accepted as a reliable method of characterisation of ionic liquid-based systems.[13] As a general comment, to date, these investigations, have focussed upon commonly-employed imidazolium-based ionic liquids. A small number of non-imidazolium-based ionic liquids have been studied using XPS.[14–19] The focus of XPS studies has mainly been upon the ionic liquid/vapour interface.[13] The most basic function of XPS of ionic liquids is confirmation of the purity; the most commonly observed impurities being silicon,[20–24] carbon[25] and oxygen,[25] which are the components of common laboratory lubricants and greases. Once purity has been established, much more subtle investigations can be carried out which may be characterised into two general areas: (*i*) the investigation of component binding energies that can elucidate electronic structure and communication (interaction) between the ionic components and (*ii*) the use of angle resolved XPS (ARXPS) to investigate surface composition and surface segregation.

XPS can be used to identify the number of electronic environments present for each element present in a sample. For ionic liquids the most common, complex and often relevant, element is carbon. Consequently, development of an understanding of the electronic environments present is vital to XPS investigations of ionic liquids. The development of a C 1s fitting model which deconstructs these different electronic environments into as small a number of components as possible is a critical goal in all XPS studies.[13,26] Binding energies provide both elemental and chemical information and

School of Chemistry, The University of Nottingham, Nottingham NG7 2RD, UK.
E-mail: peter.licence@nottingham.ac.uk; Tel: + 44 115 8466176
† Electronic supplementary information (ESI) available. See DOI: 10.1039/c1cp21053j
‡ Current E-mail: k.lovelock@ucl.ac.uk

accordingly they can be regarded as the most important pieces of raw data made available by the technique. It should be stressed that the appropriateness of the fitting model employed is crucial to the validity of processed data, and care must be taken to ensure that over-interpretation of the raw data does not occur. It should be noted at this point that the relative conductivity of the sample of interest must be considered when recording XP spectra. Surface charging has been observed in the measurement of XP spectra of some imidazolium-based ionic liquids. Unregulated or uncompensated surface charging can lead to significant shifts in the measured binding energies of XP spectra, hence charge correction using a suitable internal reference must be considered at all times. Charge correction methods aim to correct for charging phenomena post data collection. In the case of imidazolium-based ionic liquids, it was found that the peak arising from the aliphatic carbon ($C_{aliphatic}$ 1s) moiety of the ionic liquid can be used as a reliable internal reference when there were eight, or more, carbon atoms in the aliphatic chain. To charge correct ionic liquids containing shorter aliphatic chains, the peak due to the nitrogen atom of the cation (N_{cation} 1s) can be used. For a fully justified discussion of charge referencing the reader is directed to the recent article of Villar-Garcia *et al.*[26] Once reliable binding energies have been obtained, it is possible to make comparisons between ionic liquids. In particular, cation–anion interactions of both pure ionic liquids and mixtures have been probed using XPS.[26,27] These results have successfully been correlated with NMR spectroscopy,[27] theoretical calculations,[27] DSC,[28] and Kamlet–Taft parameters[27] to aid understanding of ionic liquid properties.

In this study, we investigate the XP spectra of seven 1-alkyl-1-methylpyrrolidinium-based ionic liquids (see Table 1), and also one ionic liquid mixture. The high purity of each sample is demonstrated and the electronic environment of each element present in the ionic liquids is described. In particular, a robust peak fitting model is developed for the C 1s region of $[C_nC_1Pyrr][X]$. This model is shown to be valid for all of the materials studied in this work, and we believe that it will remain valid for all structural analogues based upon the dialkylpyrrolidinium cation. Binding energy data is used to probe the magnitude of cation–anion based interactions; the effect of the anion on the electronic environment of the cation is investigated in detail for ionic liquids containing one anion and also two anions, *i.e.*, mixtures. Comparisons are made to imidazolium-based ionic liquids, in particular, a detailed comparison is made between $[C_8C_1Pyrr][X]$ and $[C_8C_1Im][X]$, where X^- is common to both ionic liquids.

Experimental

Materials

All ionic liquids investigated in this study were prepared in our laboratory using modifications to existing literature methods,[11,29,30] the structures of the liquids investigated in this study are shown in Table 1.

All ionic liquids were dried *in vacuo* ($p \leq 10^{-3}$ mbar) before being fully characterised by ^{1}H NMR, ^{13}C NMR, ESI-MS and Karl Fischer titration. Thermal data was determined by DSC (Q2000 V24.4 Build 116). When ion exchange was one of the synthetic steps, ion chromatographic analysis (both anion and cation) showed that residual ion concentrations (Cl^-, Br^-, Li^+) were all below accepted threshold concentrations, *i.e.*, <10 ppm. In all cases, no residual signals of either halide, or lithium were observed during XPS analysis, *i.e.*, the concentration was below the limit of detection. Full data, including full XPS data sets with peak deconstruction models, for all of the materials studied in this work appears in the supplementary information.†

XPS data collection

All XP spectra were recorded using a Kratos Axis Ultra spectrometer employing a focused, monochromated Al Kα source ($h\nu$ = 1486.6 eV), hybrid (magnetic/electrostatic) optics, hemispherical analyser and a multi-channel plate and delay line detector (DLD) with an X-ray incident angle of 30° (relative to the surface normal). The information depth (ID) of these experiments may be defined as the depth, within the sample, from which 95% of the measured signal will originate. ID is assumed to vary mainly with cos θ, where θ is the electron emission angle relative to the surface normal. If we assume that the inelastic mean free path (λ) of photoelectrons in organic compounds is of the order of $\sim$3 nm, at the kinetic energies employed here we can estimate ID in this geometry, when θ = 0°, ID = 7–9 nm. Consequently these data may be considered as representative of the bulk composition and do not reflect any local enhancements of concentration at the interfacial near surface region. X-ray gun power was set to 100 W. All spectra were recorded using an entrance aperture of 300 × 700 μm with a pass energy of 80 eV for survey spectra and 20 eV for high-resolution spectra. The instrument sensitivity was 7.5×10^5 counts s^{-1} when measuring the Ag $3d_{5/2}$ photoemission peak for a clean Ag sample recorded at a pass energy of 20 eV and 450 W emission power. Ag $3d_{5/2}$ full width at half maximum (FWHM) was 0.55 eV for the same instrument settings. Binding energy calibration was made using Au $4f_{7/2}$ (83.96 eV), Ag $3d_{5/2}$ (368.21 eV) and Cu $2p_{3/2}$ (932.62 eV). The absolute error in the acquisition of binding energies is ± 0.1 eV, as quoted by the instruments manufacturer (Kratos); consequently, any binding energies within 0.2 eV can be considered the same, within the experimental error. Charge neutralisation methods were not required (or employed) in the measurement of these data. Sample stubs were earthed *via* the instrument stage using a standard BNC connector.

Samples were prepared by placing a small drop ($\approx$ 20 mg) of the ionic liquid into a depression on a stainless steel sample stub (designed for powders) or on a standard stainless steel multi-sample bar (both Kratos designs). The ionic liquid samples were then cast into thin films *ex situ* (approx. thickness 0.5–1 mm), before rapid transfer to the preparative pumping chamber of the XPS instrument. Initial pumping to high vacuum pressure ($p \leq 1 \times 10^{-7}$ mbar) was carried out in the preparation chamber immediately sample preparation to ensure the complete removal of adsorbed volatiles including permanent gases, water vapour and other volatile impurities. Pumping-times varied (typically 1–3 h total) depending upon the volume, volatile impurity content and viscosity of the

Table 1 Structure and abbreviations of the ionic liquids investigated in this study

Abbreviation	Structure	Name
$[C_2C_1Pyrr][Tf_2N]$	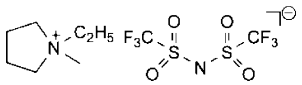	1-ethyl-1-methylpyrrolidinium bis[(trifluoromethane)sulfonyl]imide
$[C_4C_1Pyrr][Tf_2N]$	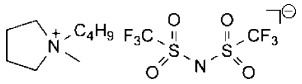	1-butyl-1-methylpyrrolidinium bis[(trifluoromethane)sulfonyl]imide
$[C_6C_1Pyrr][Tf_2N]$	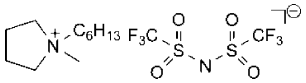	1-hexyl-1-methylpyrrolidinium bis[(trifluoromethane)sulfonyl]imide
$[C_8C_1Pyrr][Tf_2N]$	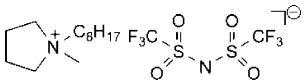	1-octyl-1-methylpyrrolidinium bis[(trifluoromethane)sulfonyl]imide
$[C_{10}C_1Pyrr][Tf_2N]$	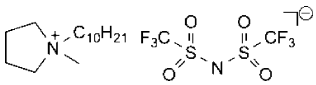	1-decyl-1-methylpyrrolidinium bis[(trifluoromethane)sulfonyl]imide
$[C_8C_1Pyrr]I$	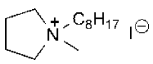	1-octyl-1-methylpyrrolidinium iodide
$[C_8C_1Pyrr][PF_6]$	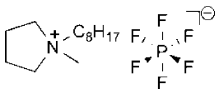	1-octyl-1-methylpyrrolidinium hexafluorophosphate
$[C_8C_1Im][Tf_2N]$	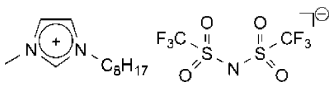	1-octyl-3-methylimidazolium bis[(trifluoromethane)sulfonyl]imide

sample, *i.e.*, viscous ionic liquids were found to require longer pumping times. The samples were then transferred to the main analytical vacuum chamber. The pressure in the main chamber remained $\leq 1 \times 10^{-8}$ mbar during XPS measurements of the samples. Pyrrolidinium–based samples were left at high vacuum for a number of days and no visual evidence of evaporation was observed. This observation strongly suggests that $[C_8nC_1Pyrr]^+$-based samples have vapour pressures significantly $\ll 1 \times 10^{-9}$ mbar at room temperature. In addition, the low chamber pressure means that all volatile impurities, such as water, are highly likely to be removed, leading to high purity samples.[31]

XPS data analysis

For data interpretation, a two point linear subtraction was used; for $[Tf_2N]^-$-based ionic liquids the C 1s XP spectra were subtracted using a linear spline to allow for the CF_3 substituent. Relative Sensitivity Factors (RSF) were taken from the Kratos Library (RSF of F 1s = 1) and were used to determine atomic percentages.[21,32] Peaks were fitted using GL(30) lineshapes; a combination of a Gaussian (70%) and Lorentzian (30%).[21,33] This lineshape has been used consistently in the fitting of XP spectra, and has been found to match experimental lineshapes in ionic liquid systems.[21,26] All XP spectra where $n = 8$ were charge corrected by setting the binding energy of the aliphatic C 1s photoemission peak ($C_{aliphatic}$ 1s) equal to 285.0 eV. For all other values of n (*i.e.*, when $n = 2, 4, 6$ and 10) spectra are charge corrected by setting the measured binding energy of the cationic nitrogen photoemission peak (N_{cation} 1s) equal to 402.7 eV. Note, 402.7 eV is the measured binding energy of the cationic nitrogen photoemission (N_{cation} 1s) in the standard reference material for this series of ionic liquids, *i.e.*, $[C_8C_1Pyrr][Tf_2N]$. This method of charge correction is valid because each of the samples in this homologous experimental series has a structurally similar cation and an identical anion, $[Tf_2N]^-$; for a full discussion of this procedure the reader is directed towards ref. 26.

To aid visual interpretation of the XP spectra presented here, all spectra are normalised to the fitted area of N_{cation} 1s,

the peak due to the nitrogen atom in the pyrrolidinium ring of $[C_8C_1Pyrr][Tf_2N]$. This peak was selected to be used for normalisation as: the N_{cation} moiety is present in all pyrrolidinium-based ionic liquids studied here in the same amount, and the binding energy is distinct from that of any other nitrogen contribution from anions studied here (or elsewhere),[13] meaning that the fit of the N_{cation} 1s peak is unequivocal. This normalisation is applied to all XP spectra for a particular ionic liquid, and therefore does not affect the relative ratios of different elements within the ionic liquid. The great benefit of this normalisation procedure is that it allows simple visual comparison of the same regions for different ionic liquids as any differences in intensity will be due to variation in the contributing chemical environments of that particular element of interest.

Results and discussion

Sample purity

Fig. 1 shows the survey XP spectrum for $[C_8C_1Pyrr][Tf_2N]$, XPS envelopes were observed for all expected elements, as was the case for each of the ionic liquids presented here. Earlier XPS studies of imidazolium-based ionic liquids have highlighted the presence of silicone-based impurities in the near-surface region that could not be detected using NMR spectroscopy or other bulk sensitive techniques.[20–24] The samples investigated in this work showed no evidence of surface segregated impurities of this type. Furthermore, there was no evidence of either Li or halide contamination carried over from ion exchange chemistries employed in synthesis, or additional hydrocarbon/oxygen impurities, in the XP spectra of any of the ionic liquids studied herein. Experimental stoichiometries, calculated from high resolution XP spectra, for each of the ionic liquids studied (seven pure ionic liquids and one ionic liquid mixture), are presented in Table 2. Experimental stoichiometries were within experimental error of nominal stoichiometries calculated from the empirical formulae of the sample.

Binding energies of $[C_nC_1Pyrr][X]$

In order to obtain absolute binding energies for components within pyrrolidinium-based ionic liquids, it is necessary to charge correct the XP spectra using an appropriate internal reference. To investigate whether such an internal reference exists for pyrrolidinium-based ionic liquids, all peaks in the XP spectra must be identified, and related to the chemical structure of the ionic liquids, *i.e.*, an appropriate multicomponent model must be applied in the deconstruction of the measured photoemission envelopes.

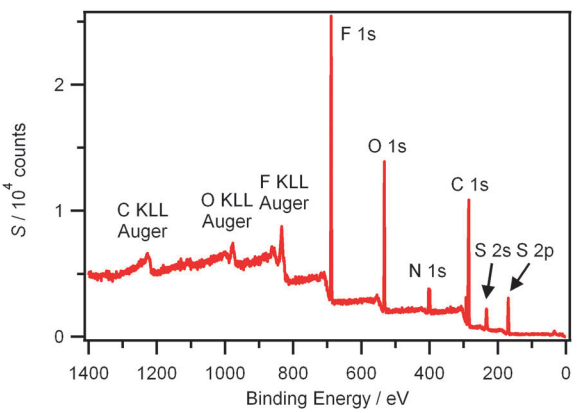

Fig. 1 Survey XP spectrum for $[C_8C_1Pyrr][Tf_2N]$.

The electronic environment of carbon, the development of a fitting model

Identification and assignment of the electronic environments that contribute towards the C 1s region of the XP spectra for ionic liquid-based samples is vital. At first sight, it is clear that there are three contributions, two of which are not fully resolved, that combine to give the experimental C 1s XP spectra for $[C_nC_1Pyrr][Tf_2N]$, where n = 2–10, and two unresolved peaks for both $[C_8C_1Pyrr][PF_6]$ and $[C_nC_1Pyrr]I$ (Fig. 2). For $[C_nC_1Pyrr][Tf_2N]$, the peak at highest binding energy ($\approx$ 293.0 eV) is assigned to the CF_3 group of the anion, as assigned previously for a wide range of imidazolium-based ionic liquids.[21,24] The two peaks at binding energies 286.4–286.8 eV and $\approx$ 285 eV are due to the carbon components within $[C_nC_1Pyrr]^+$. From an assessment of the chemical structure of $[C_nC_1Pyrr]^+$, (Fig. 2) there are at least two different chemical environments. The first of these two environments is carbon bonded to nitrogen; $[C_nC_1Pyrr]^+$ contain four such atoms, labelled (C^2 + C^5 + C^6 + C^7). The second environment is carbon bonded to carbon and hydrogen only; the magnitude of this component varies, depending upon n. For example, for $[C_{10}C_1Pyrr][Tf_2N]$ there are 11 such carbon atoms, two in the pyrrolidinium ring, labelled (C^3 + C^4) and nine in the C_{10} alkyl substituent, labelled (C^8 through C^{16}). As these two, well-defined contributions are consistent with a theoretical model, a two-component fitting model was initially considered. However, a two-component fitting model was found to be unsatisfactory when $n \geq 4$. The FWHM for combined (C^2 + C^5 + C^6 + C^7) remains effectively constant as n increases from 4 to 10 (1.02 $\pm$ 0.03 eV), whereas for the component corresponding to (C^3 + C^4 + C^8 through C^{n+6}) the FWHM increases as n increases, *i.e.*, the FWHM ratio for these components increases with increasing n. This trend shows that as more carbon atoms are added to the chain, the variation in the electronic environment of the aliphatic carbons increases also. Generally, the carbon atoms located further away from the positively charged nitrogen atom are expected to be less positively charged, and therefore more like "normal" aliphatic carbons, *i.e.*, like carbons in simple molecules such as hexane. Upon closer inspection, it becomes clear that in the case of samples with smaller values of n, the components modelled as (C^3 + C^4 + C^8 through C^{n+6}) gave rise to a binding energy that is not characteristic of typical aliphatic carbon atoms. Clearly the close proximity of these carbon atoms to the nitrogen of the cation reduced their electron density and shifted their photoemission peak to a slightly higher binding energy. It was subsequently decided that a two-component model for C 1s was too simple and was not able to produce reliable binding energies for aliphatic carbon across a range of samples with variable n. Further details on the two-component fitting model are given in the Supporting Information, Section S3.

Table 2 Measured experimental and nominal (in brackets) stoichiometries for the ionic liquids studied in this work. RSF = relative sensitivity factors, taken from ref. 21 and 32

Anion [X] $[C_nC_1Pyrr][X]$	n	RSF	C 1s 0.278	N 1s 0.477	O 1s 0.780	F 1s 1.000	S 2p 0.668	P 2p 0.486	I 3d 10.343
$[Tf_2N]^-$	2	Measured (nominal)	9.8 (9.0)	2.1 (2.0)	3.3 (4.0)	6.3 (6.0)	1.4 (2.0)		
	4	Measured (nominal)	11.5 (11.0)	1.9 (2.0)	3.4 (4.0)	6.5 (6.0)	1.7 (2.0)		
	6	Measured (nominal)	13.5 (13.0)	1.9 (2.0)	3.5 (4.0)	6.4 (6.0)	1.7 (2.0)		
	8	Measured (nominal)	15.7 (15.0)	1.9 (2.0)	3.5 (4.0)	6.3 (6.0)	1.7 (2.0)		
	10	Measured (nominal)	17.6 (17.0)	1.9 (2.0)	3.5 (4.0)	6.4 (6.0)	1.7 (2.0)		
$[PF_6]^-$	8	Measured (nominal)	14.0 (13.0)	0.9 (1.0)		5.2 (6.0)		0.9 (1.0)	
I^-	8	Measured (nominal)	12.9 (13.0)	1.0 (1.0)					1.1 (1.0)
$[Tf_2N]^-:I^-$ (1 : 1)	8	Measured (nominal)	14.5 (14.0)	1.4 (1.5)	1.8 (2.0)	3.1 (3.0)	0.7 (1.0)		0.4 (0.5)

Clearly the unsuitability of a simple two-component model signalled the requirement for the inclusion of a third component that could reflect the change in electron density, associated with each carbon, as the distance from nitrogen increases. In principle each carbon atom may feel a slightly lower "pull" on its bonding electrons as the distance between the carbon and the electropositive nitrogen increases. However, the inclusion of an additional n-1 contributions would overcomplicate the model and render it practically useless. In practice, the aliphatic carbon contribution was efficiently fit with the addition of only one more component. Consequently, the $[C_nC_1Pyrr]^+$ C 1s region was reliably fit with a good agreement, across all values of n investigated ($2 \leq n \leq 10$), to a three-component model. The three separate C 1s components, or chemical environments, of $[C_nC_1Pyrr]^+$ are shown in Fig. 2. C_{hetero} represents the carbon atoms bonded directly to a nitrogen atom, also labelled (C^2 + C^5 + C^6 + C^7) in Fig. 2. All $[C_nC_1Pyrr]^+$-containing ionic liquids studied have four C_{hetero} atoms. C_{inter} represents so-called "intermediate" carbon atoms that are bonded to carbon, which is then in term bonded to nitrogen, *i.e.*, β to the cationic nitrogen; these contributions are labelled (C^3 + C^4 + C^8) in Fig. 2. Every $[C_nC_1Pyrr]^+$ contains three C_{inter} atoms. The final contribution, $C_{aliphatic}$, represents the remaining carbon atoms that are located in purely aliphatic environments, *i.e.* bonded to carbon and also β to carbon; $C_{aliphatic}$ includes (C^9 through C^{n+6}), depending upon the length of n.

The constraints used in the development of the three-component fitting model will now be explained in detail. To begin with, the focus will be upon $[C_2C_1Pyrr][Tf_2N]$, which contains no $C_{aliphatic}$. The nominal stoichiometry for $[C_2C_1Pyrr][Tf_2N]$ is $C_{hetero}:C_{inter}$ = 4 : 3. When fitting the C 1s region for $[C_2C_1Pyrr][Tf_2N]$ with two components the area ratio was constrained to 4 : 3; a very satisfactory fit was achieved (Fig. 2). The full width at half maxima (FWHM) for the two components were very similar, giving a ratio of 1 : 1.03, confirming that there are two distinct carbon electronic environments for $[C_2C_1Pyrr][Tf_2N]$. An accurate value for binding energy (C_{hetero} 1s − C_{inter} 1s) = 1.27 eV was obtained.

For the three-component fitting model for $n \geq 4$, it is necessary to constrain the component areas, the FWHM (C_{hetero} 1s constrained to be equal to C_{inter} 1s) and the binding energy separation of (C_{hetero} 1s − C_{inter} 1s) = 1.27 eV, as it is assumed that the relative electronic environments of C_{hetero} and C_{inter} will not change significantly as n increases. Application of these constraints gave rise to satisfactory fits when $n \geq 4$, further justifying truncation of the fit to only three-components. It is important to note that the FWHM ratio of ($C_{aliphatic}$ 1s) : (C_{hetero} 1s) was ≈ 1.1 when n = 4–10, indicating that the carbon atoms labelled $C_{aliphatic}$, *i.e.*, C^9 to C^{16}, are all in very similar electronic environments. Clearly, these carbon atoms are located sufficiently far away from the electropositive nitrogen atom to be relatively uninfluenced by it.

The binding energy separation for C_{hetero} 1s and C_{inter} 1s is expected to vary as the nature of the anion changes; this variation will be explored in detail in later sections. As neither $[C_2C_1Pyrr][PF_6]$ nor $[C_2C_1Pyrr]I$ were studied, a definitive binding energy separation for C_{hetero} 1s and C_{inter} 1s for these anions is not available at this time; this separation is the subject of on-going investigations. Accordingly, no constraint was applied to the binding energy separation in these cases. The key assumption employed to obtain a satisfactory fit for the three-component fitting model was that the FWHM ratio of ($C_{aliphatic}$ 1s) : (C_{hetero} 1s) was ≈ 1.1, as determined for $[C_nC_1Pyrr][Tf_2N]$ where n = 4–10. Application of this constraint, along with area constraints, yielded a satisfactory fit for the two samples studied here. The binding energy separations (C_{hetero} 1s − C_{inter} 1s) = 1.21 eV and 1.07 eV for $[C_8C_1Pyrr][PF_6]$ and $[C_8C_1Pyrr]I$ respectively (for the 1 : 1 mixture of $[C_8C_1Pyrr][Tf_2N]$ and $[C_8C_1Pyrr]I$ the separation is 1.17 eV).

Electronic environment of nitrogen and other anion associated regions

The N 1s XP spectra for $[C_nC_1Pyrr][Tf_2N]$, where n = 2–10, all contain two characteristic and clearly resolved peaks; the N 1s XP spectra for $[C_8C_1Pyrr][PF_6]$ and $[C_8C_1Pyrr]I$ both contain a single peak, (see Fig. S6 and S7†). The peak at higher binding energy, 402.4 to 402.7 eV, is assigned to the nitrogen atom from the pyrrolidinium ring, and is labelled N_{cation} 1s. The peak at lower binding energy for $[C_nC_1Pyrr][Tf_2N]$, ≈ 399.5 eV, is assigned to the nitrogen atom from the $[Tf_2N]^-$ anion, labelled N_{anion} 1s; this binding energy is comparable with that observed for a range of $[C_nC_1Im][Tf_2N]$ ionic liquids.[21,24,26] As the binding energy of N_{cation} 1s is larger than N_{anion} 1s by ≈ 3.2 eV, we can unequivocally state that N_{cation} is significantly more electropositive than N_{anion}. The (N_{cation} 1s) : (N_{anion} 1s) peak intensity ratio is ≈ 1 : 1 for all $[C_nC_1Pyrr][Tf_2N]$ ionic liquids investigated at θ = 0°, matching the nominal stoichiometry.

The fluorine, oxygen and sulfur regions for $[C_nC_1Pyrr][Tf_2N]$ each show a single electronic environment, which is

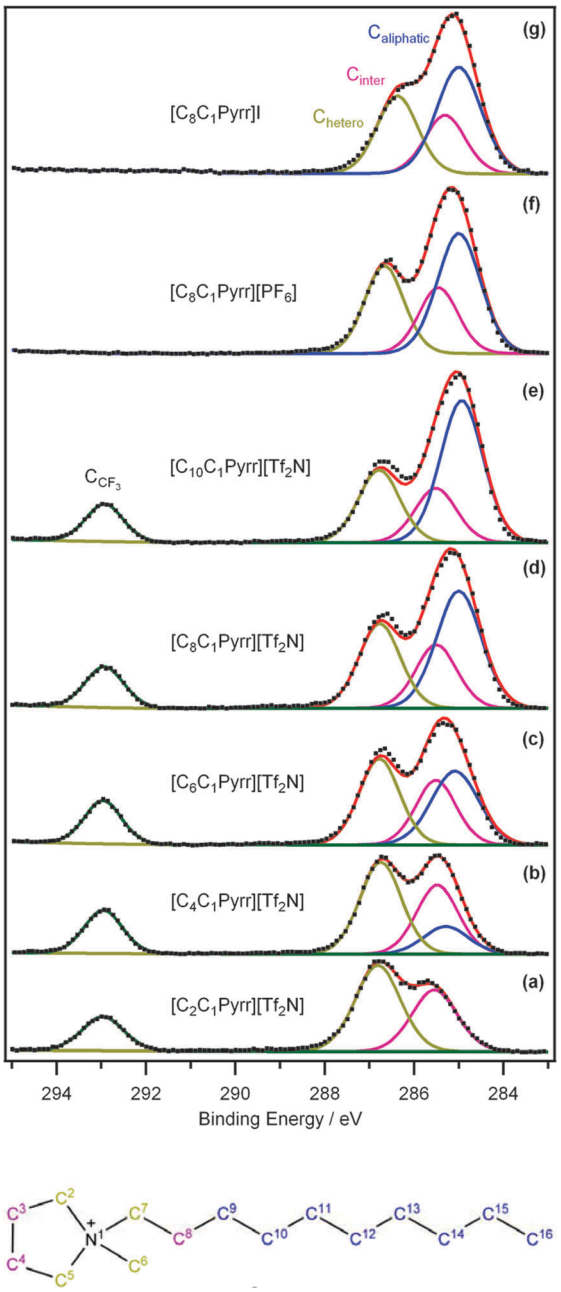

Fig. 2 C 1s XP spectra with component fittings for (a) $[C_2C_1Pyrr][Tf_2N]$, (b) $[C_4C_1Pyrr][Tf_2N]$, (c) $[C_6C_1Pyrr][Tf_2N]$, (d) $[C_8C_1Pyrr][Tf_2N]$, (e) $[C_{10}C_1Pyrr][Tf_2N]$, (f) $[C_8C_1Pyrr][PF_6]$, (g) $[C_8C_1Pyrr]I$. The intensities are normalised to the intensity of the N_{cation} 1s fitted peak for $[C_8C_1Pyrr][Tf_2N]$. All XP spectra when $n = 8$ are charge corrected by referencing the aliphatic C 1s photoemission peak ($C_{aliphatic}$ 1s) to 285.0 eV. When $n = 2$, 4, 6 and 10, all XP spectra are charge corrected by referencing to N_{cation} 1s which was recorded for the standard $[C_8C_1Pyrr][Tf_2N]$ (402.7 eV). $[C_{10}C_1Pyrr][Tf_2N]$ labelled structure: $(C^2 + C^5 + C^6 + C^7) = C_{hetero}$ (yellow), $(C^3 + C^4 + C^8) = C_{inter}$ (mauve) and (C^9 to C^{16}) = $C_{aliphatic}$ (blue).

in agreement to earlier XPS studies of $[C_nC_1Im][Tf_2N]$ (see Supporting Information, Fig. S1 to S5†).[21,24,26] The six fluorine atoms are indistinguishable by XPS, and the same is true for the four oxygen atoms and two sulfur atoms. It should be noted that the observed doublet of the S 2p photoemission is entirely due to spin–orbit splitting into the S $2p_{1/2}$ and S $2p_{3/2}$ levels (in an area ratio of 1 : 2), and does not signify the presence of two distinct environments. For $[C_8C_1Pyrr][PF_6]$, the F 1s XP spectrum gives a single peak, showing that all six fluorine atoms are indistinguishable by XPS (see Supporting Information, Fig. S6†), and the P 2p spectrum shows two peaks due to spin-orbit coupling (in an area ratio of 1 : 2); only one phosphorus electronic environment was observed.[26,34] For $[C_8C_1Pyrr]I$, the I 3d spectrum shows two peaks separated by $\approx$ 11.5 eV (in an area ratio of 2 : 3); these peaks are also due to spin-orbit coupling (see Supporting Information, Fig. S7†), again only a single environment is observed.[26,34]

The measurement of accurate binding energies and the effect of aliphatic chain length on binding energies

In the previous section we described the development of a robust three-component fitting model for the C 1s region of ionic liquids of the general $[C_nC_1Pyrr][X]$. The binding energies obtained for the $C_{aliphatic}$ 1s component of this fit can be used as a robust internal charge reference by setting the observed $C_{aliphatic}$ 1s component equal to 285.0 eV. All other regions are subsequently shifted by the same amount as the $C_{aliphatic}$ 1s component. The binding energy of N_{cation} 1s for $n = 8$, 402.7 eV, can then be used to charge correct all other $[C_nC_1Pyrr][X]$ ionic liquids, *i.e.*, where $n = 2$, 4, 6, 10, as the electronic environment of the cation nitrogen is not expected to vary with n, as long as $[X]^-$ is unchanged. Fig. 3a and b show the charge corrected C 1s and N 1s XP spectra for $[C_nC_1Pyrr][Tf_2N]$. All binding energies remain constant as n varies, apart from the $C_{aliphatic}$ 1s component (Fig. 3c). The conclusion is that the length of the aliphatic chain makes little or no difference to the interaction of the charge-bearing head groups of the cation and anion, and therefore to their electronic interaction, confirming the validity of using N_{cation} 1s for charge referencing. This finding is in agreement with the decomposition of enthalpies of vaporisation at 298 K, $\Delta_{vap}H_{298}$, for a range of ionic liquids, including $[C_nC_1Pyrr][Tf_2N]$ where $n = 4$–8, which suggests that the coulombic contribution does not change significantly when n changes and the anion is the same.[11,36] For $n = 8$ and 10, the binding energies of $C_{aliphatic}$ 1s are the same, within the error of the experiment. This observation shows that the $C_{aliphatic}$ 1s component for these ionic liquids is a good representation of aliphatic carbon. For $n = 6$, the binding energy of $C_{aliphatic}$ 1s increases relative to $n = 8$, but still within the error of the experiment. For $n = 4$, clearly the binding energy of the $C_{aliphatic}$ 1s component increases significantly relative to $n = 8$, indicating that the two aliphatic carbons for $[C_4C_1Pyrr][Tf_2N]$ are much more electropositive than the aliphatic carbon atoms further away from the nitrogen atom. This difference is due to the relative distance of the carbon atoms from the electropositive nitrogen atom. Therefore, $C_{aliphatic}$ 1s for $n = 4$ cannot be used for satisfactory charge correction, whereas for $C_{aliphatic}$ 1s for $n \geq 6$ can be used. Throughout this contribution, the binding energy of $C_{aliphatic}$ 1s for $n = 8$ was set to 285.0 eV. As the binding energy for N_{cation} 1s is

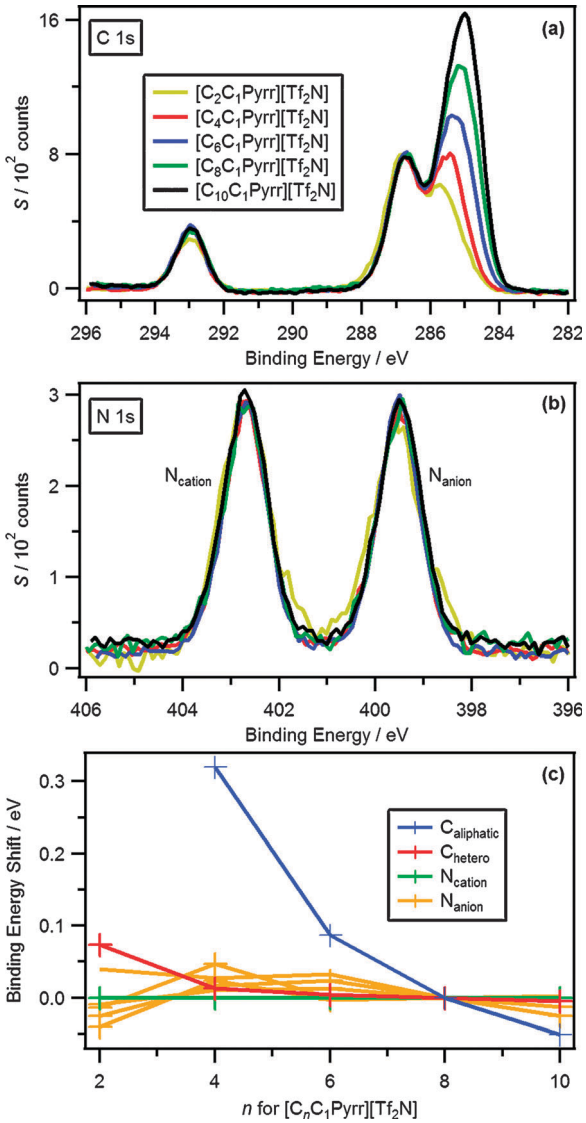

Fig. 3 XP spectra for $[C_nC_1Pyrr][Tf_2N]$ where n = 2–10 for: (a) C 1s and (b) N 1s. The intensities are normalised to the intensity of the N_{cation} 1s fitted peak for $[C_8C_1Pyrr][Tf_2N]$. For n = 8, XP spectra were charge corrected by referencing the aliphatic C 1s photoemission peak ($C_{aliphatic}$ 1s) to 285.0 eV. For other n values, XP spectra were charge corrected by referencing the N_{cation} 1s to the value for n = 8. (c) Binding energy shifts relative to $[C_8C_1Pyrr][Tf_2N]$ as a function of aliphatic chain length, n = 2–10. It should be noted that the experimental error associated with the measurement of binding energies is of the order ± 0.1 eV.

unaffected by n, this value was used for charge correction of $[C_nC_1Pyrr][Tf_2N]$, where n = 2, 4, 6, 10. It is recommended that such a procedure is used within ionic liquid families, *i.e.*, ionic liquids where the n is different but the anion is the same. As the binding energies are charge corrected, the data presented in Table 3 may find future use as a standard list of binding energies for $[C_nC_1Pyrr][X]$ ionic liquids. In particular, if ionic liquids such as $[C_nC_1Pyrr][PF_6]$ are studied using XPS, the XP spectra can be charge corrected to the binding energy of N_{cation} 1s, 402.5 eV, for $[C_8C_1Pyrr][PF_6]$. Similarly, N_{cation} 1s, 402.4 eV, for $[C_8C_1Pyrr]I$ can be used for charge correction of $[C_nC_1Pyrr]I$.

The observation that changing n does not affect the electronic interaction between the cation and anion is reinforced by analysis of $\Delta_{vap}H_{298}$ values for $[C_nC_1Pyrr][Tf_2N]$, where n = 4, 6, 8. $\Delta_{vap}H_{298}$ which can be broken down into two components, the coulombic contribution, $E_{coul,}$ and the van der Waals contribution, E_{vdW}.[11,36] For n = 4–8, E_{coul} is approximately constant (71 to 74 kJ mol^{-1}), whereas E_{vdW} increases from 78 kJ mol^{-1} for n = 4, to 90 kJ mol^{-1} for n = 8. In combination with the XPS results, the suggestion is that the electrostatic interaction for $[C_nC_1Pyrr][Tf_2N]$ does not vary with n, and any variation in properties with n is due to changes in the van der Waals interactions.

Effect of the cation on the anion: $[C_8C_1Pyrr][X]$ versus $[C_8C_1Im][X]$

Having obtained reliable and reproducible binding energies for all $[C_nC_1Pyrr][X]$ ionic liquids, comparisons can now be made between binding energies of pyrrolidinium-based ionic liquids and imidazolium-based ionic liquids. A visual comparison between $[C_8C_1Pyrr][Tf_2N]$ and $[C_8C_1Im][Tf_2N]$ for all regions is given in Fig. 4. The XP spectra are all charge corrected to the binding energy of $C_{aliphatic}$ 1s, and are normalised to the area of the F 1s component, as both ionic liquids contain six fluorine atoms. The first observation is that the relative areas of the components agree well, *e.g.*, S 2p, O 1s, C_{CF3} 1s, N_{anion} 1s, confirming the validity of normalising the areas of the spectra. The second, more important, observation is that the binding energies of all anionic components match, within the error of the experiment (Fig. 4a–e and Table 3). For example, F 1s for $[C_8C_1Pyrr][Tf_2N]$ is 688.9 eV and for $[C_8C_1Im][Tf_2N]$ is 688.8 eV. In addition, for $[C_8C_1Pyrr][PF_6]$ and $[C_8C_1Im][PF_6]$, the binding energies of the P $2p_{3/2}$ and F 1s components are the same (136.6 eV and 686.6/686.7 eV respectively). For $[C_8C_1Pyrr]I$ and $[C_8C_1Im]I$, the measured I $3d_{5/2}$ peaks are also constant, within the experimental error (618.4/618.5 eV). These observations indicate that changing the cation from imidazolium to pyrrolidinium has relatively little effect on the electronic environment of the anion.

Comparing the binding energies of the peaks due to the cations, Fig. 4b and f, reveals significant differences. The binding energies of N_{cation} 1s for $[C_8C_1Pyrr][Tf_2N]$ and $[C_8C_1Im][Tf_2N]$ are 402.7 eV and 402.1 eV respectively, see Fig. 4b. In general, N_{cation} 1s binding energies for $[C_8C_1Pyrr][X]$ (where X = $[Tf_2N]^-$, $[PF_6]^-$ and I^-) are significantly higher than those for $[C_8C_1Im][X]$, 0.5 ± 0.1 eV. This observation shows that the nitrogen atom in $[C_8C_1Pyrr][X]$ is significantly more electropositive than the nitrogen atoms in $[C_8C_1Im][X]$. The binding energies of the carbon atoms within the cation can also be compared. Clearly, $[C_8C_1Im][Tf_2N]$ contains a C 1s cation component at higher binding energy than $[C_8C_1Pyrr][Tf_2N]$, Fig. 4f. Our group have previously established that for $[C_nC_1Im][X]$, the component at highest binding energy is due to the carbon of the imidazolium ring bonded to two nitrogen atoms, *i.e.*, at the C^2 position of the imidazolium ring.[21,26] The C^2 atom of imidazolium is more electropositive than the C_{hetero} atoms of pyrrolidinium. For example, the binding energy of the C^2 component for $[C_8C_1Im][Tf_2N]$ is 287.7 eV,[26] whereas C_{hetero} 1s for $[C_8C_1Pyrr][Tf_2N]$

Table 3 Binding energies in eV for all regions for $[C_nC_1Pyrr][X]$ and for all regions for $[C_8C_1Im][X]$ (taken from ref. 26 and 35). It should be noted that the experimental error associated with the measurement of binding energies is of the order ± 0.1 eV

Ionic liquid		Binding energy (eV)										
Cation	Anion	$C_{aliphatic}$ 1s	C_{inter} 1s	C_{hetero} 1s	N_{cation} 1s	C_{CF3} 1s	N_{anion} 1s	O 1s	F 1s	S $2p_{3/2}$	P $2p_{3/2}$	I $3d_{5/2}$
$[C_2C_1Pyrr]^+$	$[Tf_2N]^-$		285.5	286.8	402.7	293.0	399.4	532.6	688.9	169.0		
$[C_4C_1Pyrr]^+$	$[Tf_2N]^-$	285.3	285.5	286.8	402.7	293.0	399.5	532.7	688.9	169.0		
$[C_6C_1Pyrr]^+$	$[Tf_2N]^-$	285.1	285.5	286.8	402.7	293.0	399.5	532.7	688.9	169.0		
$[C_8C_1Pyrr]^+$	$[Tf_2N]^-$	285.0	285.5	286.8	402.7	292.9	399.5	532.7	688.9	169.0		
$[C_{10}C_1Pyrr]^+$	$[Tf_2N]^-$	284.9	285.5	286.8	402.7	292.9	399.5	532.7	688.9	169.0		
$[C_8C_1Pyrr]^+$	$[PF_6]^-$	285.0	285.5	286.7	402.5				686.6		136.6	
$[C_8C_1Pyrr]^+$	I^-	285.0	285.3	286.4	402.4							618.4
$[C_8C_1Pyrr]^+$	$[Tf_2N]^-:I^-$ [a]	285.0	285.4	286.5	402.5	292.9	399.5	532.6	688.9	168.9		618.4
$[C_8C_1Im]^+$	$[Tf_2N]^-$ [b]	285.0			402.1	292.9	399.5	532.7	688.8	169.0		
$[C_8C_1Im]^+$	$[PF_6]^-$ [b]	285.0			402.1				686.7		136.6	
$[C_8C_1Im]^+$	I^- [b]	285.0			401.9							618.5
$[C_8C_1Im]^+$	I^- [c]	285.0			401.8							618.5

[a] Molar ratio of $[Tf_2N]^-:I^-$ was 1 : 1. [b] Taken from ref. 26. [c] Taken from ref. 35.

is 286.8 eV. The binding energies for the two components for $[C_8C_1Im][Tf_2N]$ due to the other C_{hetero} atoms (labelled as (C^4 + C^5) and (C^6 + C^7), see supporting information, Fig. S8†) are 286.6 eV and 287.0 eV.[26] These values are very similar to the C_{hetero} 1s binding energy for $[C_8C_1Pyrr][Tf_2N]$, 286.8 eV, suggesting that the C_{hetero} 1s for $[C_8C_1Pyrr][Tf_2N]$ is in a similar electronic environment to the two components (C^4 + C^5) and (C^6 + C^7) for $[C_8C_1Im][Tf_2N]$. A key reason that pyrrolidinium-based ionic liquids have received such interest for electrochemistry-based applications is their greater cathodic stability than imidazolium-based ionic liquids with regard to cation reduction.[37] The differences in stability have been related to the ease of removal of the C^2 proton of the imidazolium cation.[37–41] The XPS results here confirm that the C^2 carbon in imidazolium is in general more electropositive than any carbon atom in pyrrolidinium, supporting the assertion that pyrrolidinium-based ionic liquids have greater cathodic stability.

Anion–cation interactions, pure $[C_8C_1Pyrr][X]$ based ionic liquids and ionic liquid mixtures

Previous studies have suggested that anion-cation interactions can be investigated by XPS.[27,28,42] The binding energies of C_{hetero} 1s and N_{cation} 1s have been shown to correlate with the anion basicity; for low basicity anions such as $[Tf_2N]^-$, the binding energies are relatively high, meaning that the cation is relatively electropositive. Clearly, low basicity anions transfer relatively little charge to the cation; the opposite is true for high basicity anions such as Cl^- and I^-.

The effect of the anion on the electronic environment of the cation has been investigated for three $[C_8C_1Pyrr][X]$ ionic liquids, where X = $[Tf_2N]^-$, $[PF_6]^-$ and I^- (Fig. 5). The XP spectra of all regions are charge corrected to $C_{aliphatic}$ 1s = 285.0 eV. The areas are normalised to the area of N_{cation} 1s. It must be noted that the FWHM of the N_{cation} 1s peak for $[C_8C_1Pyrr][PF_6]$ is slightly larger than for the other two ionic liquids. This difference is because $[C_8C_1Pyrr][PF_6]$ is a solid under the XPS conditions (UHV, ≈300 K). As a result, it is likely that charging occurred during the measurement of XP data. Surface charging of insulators can lead to a moderate broadening of the photoemission envelopes for each element investigated. Similarly the measured binding energy of the photoemissions has also been observed to shift by an amount which is, in some way, proportional to the magnitude of the charge located at the sample surface. The impact of charging is a function of structure and relative conductivity of each sample under consideration.[21,26] However, as the XP spectra in this study are charge corrected to an internal reference peak, *i.e.* $C_{aliphatic}$ 1s, the binding energies are expected to be reliable. The binding energies for both N_{cation} 1s and C_{hetero} 1s follow the trend: $[Tf_2N]^-$ > $[PF_6]^-$ > I^-, with higher binding energies corresponding to more electropositive cations. This trend may be interpreted as increased charge transfer from the anion to the cation, especially in the case of more basic anions, *e.g.*, I^-. These data show a similar trend to analogous experiments comparing a range of imidazolium-based ionic liquids.[27,28,42] The Kamlet–Taft parameter, β, which is a measure of hydrogen bond acceptor ability, has been measured for a restricted set of pyrrolidinium-based ionic liquids.[43,44] Sadly, at this time, an insufficient number of samples have been studied to allow valid comparisons to be made to the binding energy data presented here. However, based upon the strong linear correlation between β and N_{cation} 1s binding energies exhibited for imidazolium-based ionic liquids, it is expected that for pyrrolidinium-based ionic liquids β values will follow a similar trend.

Mixtures of ionic liquids have previously been studied using XPS to investigate both surface composition[45] and subtle changes in component binding energies as a result of the different electronic environment within the mixture.[28] The surface composition study showed that a mixture of ionic liquids still results in the nominal stoichiometry of the combined ions at the surface (ID = 1–1.5 nm), suggesting that the bulk electronic environment of the ionic liquid mixture can effectively be probed using XPS at θ = 0° (ID = 7–9 nm).[45] For imidazolium-based ionic liquids, the binding energies of specific ions (*i.e.*, the components within that ion) within mixtures have been shown to vary when compared to those of the same ion in pure, simple ionic liquids.[28]

A 1 : 1 mixture of $[C_8C_1Pyrr][Tf_2N]:[C_8C_1Pyrr]I$ was selected for investigation based upon two specific sets of criteria:

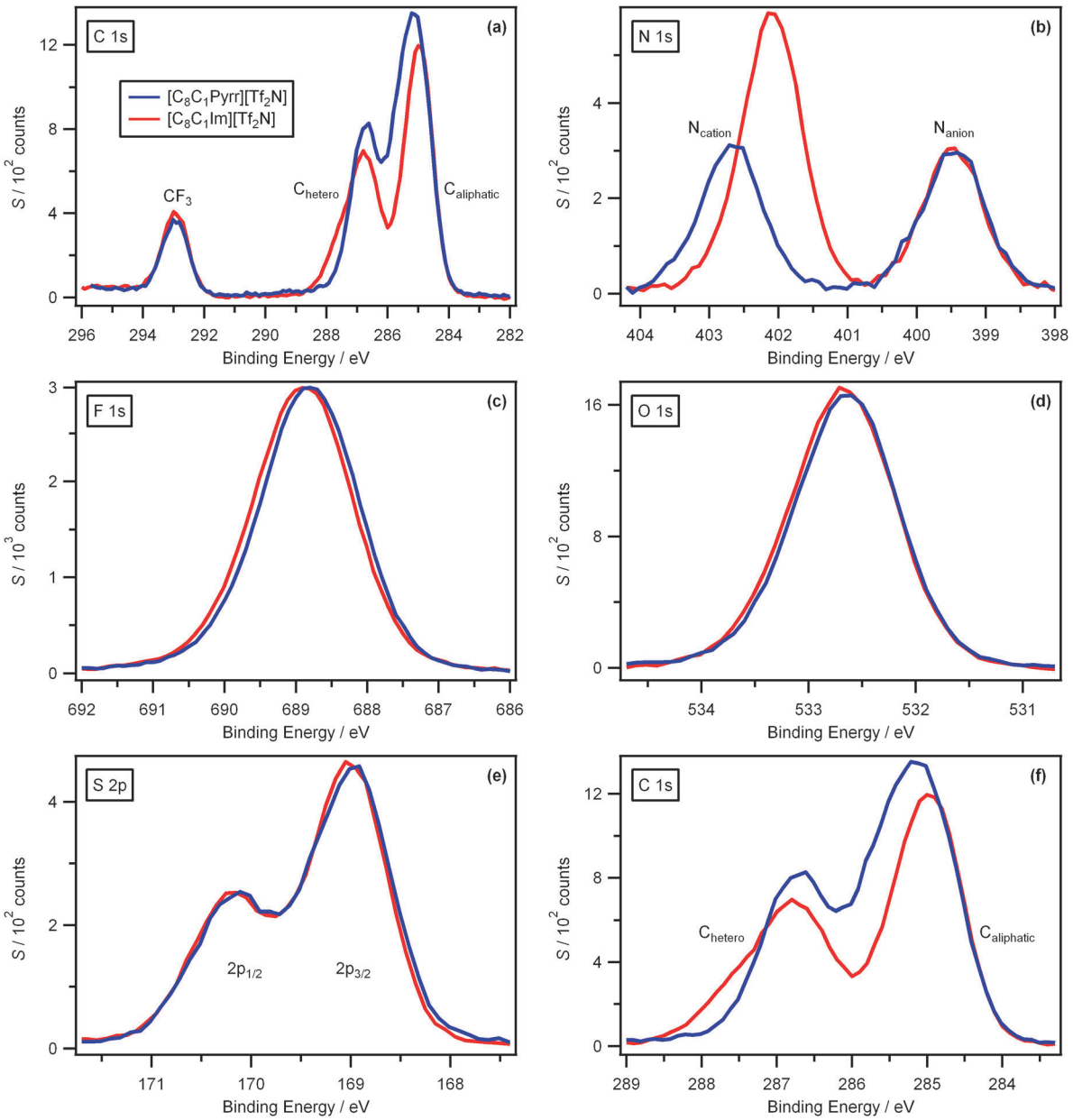

Fig. 4 XP spectra of $[C_8C_1Pyrr][Tf_2N]$ and $[C_8C_1Im][Tf_2N]$ for: (a) C 1s, (b) N 1s, (c) F 1s, (d) O 1s, (e) S 2p and (f) C 1s with truncated *x*-axis to show the cation region only. The intensities are normalised to the intensity of the F 1s peak for $[C_8C_1Pyrr][Tf_2N]$. All XP spectra were charge corrected by referencing the aliphatic C 1s photoemission peak ($C_{aliphatic}$ 1s) to 285.0 eV.

primarily both pure ionic liquids have been previously studied, and secondly because the anions have relatively different basicities. The differences in basicity of the anions is sufficiently large such that the differences in binding energies of C_{hetero} 1s and N_{cation} 1s are larger than the systematic error within the experiment. A common $[C_8C_1Pyrr]^+$ cation was chosen to reduce the number of variables and allow accurate charge referencing of the system. XP spectra for C 1s, N 1s and I $3d_{5/2}$ for the mixture and the pure ionic liquids are shown in Fig. 6. The binding energies of the XP spectra are charge corrected to the predetermined value of $C_{aliphatic}$ 1s = 285.0 eV, and the areas are normalised to the area of N_{cation} 1s to aid visual comparisons to be made. The binding energies of the cationic components, C_{hetero} 1s and N_{cation} 1s, in the mixture are observed at binding energies between those of the two pure ionic liquids (Fig. 7a and b respectively). Interestingly, the peaks for N_{anion} 1s and I $3d_{5/2}$ show no such change in binding energy and are identical to those in the pure ionic liquids (Fig. 7d and c respectively). These results show that the electronic environment of the cation can be tuned to a desired value by manipulation of the anion composition within a mixture, with very little impact upon the anion itself, within the error of these measurements. It is vital to point out that the FWHM of N_{cation} 1s for the mixture is similar to that for the pure ionic liquids. This observation demonstrates that, in the mixture, the cation is in a single electronic environment, not a mixture of two electronic environments (such a scenario would likely give rise to a single peak with a

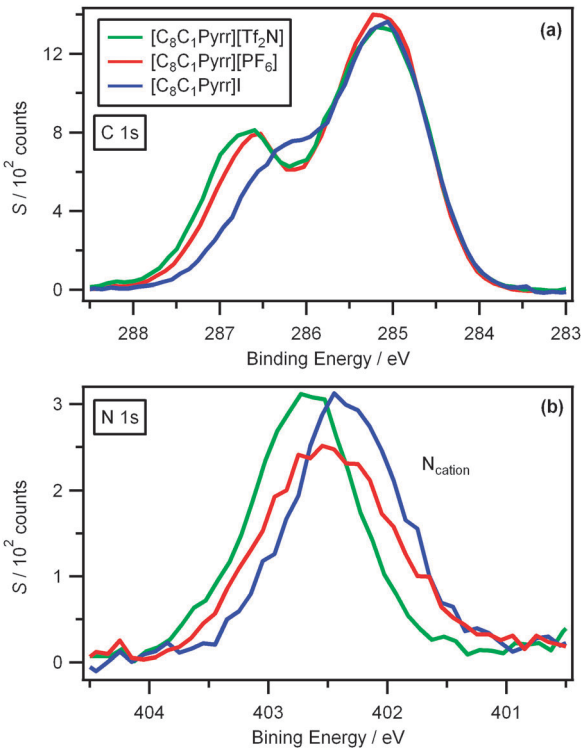

Fig. 5 XP spectra for $[C_8C_1Pyrr][Tf_2N]$, $[C_8C_1Pyrr][PF_6]$ and $[C_8C_1Pyrr]I$ for: (a) C 1s, (b) N 1s. The intensities are normalised to the intensity of the N_{cation} 1s fitted peak for $[C_8C_1Pyrr][Tf_2N]$. All XP spectra were charge corrected by referencing the aliphatic C 1s photoemission peak ($C_{aliphatic}$ 1s) to 285.0 eV. Note, to allow simple comparisons to be made, the binding energy scale of the experimental C 1s spectrum is truncated to show the cation region only, *i.e.* the CF_3 component of $[Tf_2N]^-$ is not displayed.

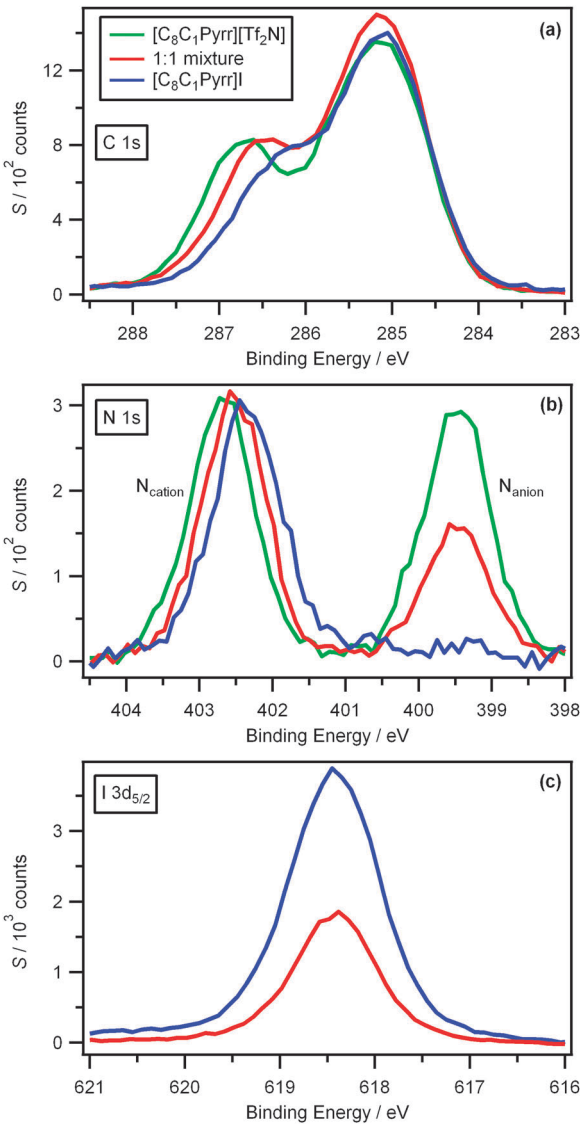

Fig. 6 XP spectra for a 1 : 1 mixture of $[C_8C_1Pyrr][Tf_2N]$: $[C_8C_1Pyrr]I$ and pure ionic liquids $[C_8C_1Pyrr][Tf_2N]$ and $[C_8C_1Pyrr]I$ for: (a) C 1s, (b) N 1s and (c) I $3d_{5/2}$. All XP spectra were charge corrected by referencing the aliphatic C 1s photoemission peak ($C_{aliphatic}$ 1s) to 285.0 eV. Note to allow simple comparisons to be made, the binding energy scale of the experimental C 1s spectrum is truncated to show the cation region only, *i.e.* the CF_3 component of $[Tf_2N]^-$ is not displayed.

significantly larger FWHM than those of the pure ionic liquids). The conclusion is that the ionic liquid mixture contains an intimate mixture of cations and randomly distributed anions, not discrete pockets of the cation and one type of anion or the other. This experiment does not support, or disprove, the formation of polar and non-polar domains within pyrrolidinium-based ionic liquids, but it does eliminate the formation of discrete pockets of different ionic liquids within the bulk ionic liquid mixture, as would be the case in an aggregate or emulsion-based system.

Overall the results for both pure $[C_8C_1Pyrr][X]$ and indeed the mixture shows that the anion can significantly influence the electronic environment of the cation. This knowledge can be used to tune the electronic environment of the cation, in particular by using the appropriate mixture of different anions. This method could, in principle, deliver a material with a very specific series of physical and chemical properties.

Surface tension measurements for $[C_nC_1Pyrr][Tf_2N]$, where n = 3–10, show the surface tension decreased with increasing n;[46] a similar trend has been observed for imidazolium-based ionic liquids.[47] At first glance, it may appear that a simple correlation exists between the surface tension and the amount of aliphatic carbon present at the outer surface. However, such a simple correlation has been shown not to exist when a wider variety of imidazolium-based ionic liquids is considered.[47] Surface tension is determined by the balance of two factors: the intermolecular energy (*i.e.*, the cohesive energy density, CED) and the orientation of molecules at the surface.[47] The CED is directly related to $\Delta_{vap}H_{298}$.[48] It was explained previously, using XPS binding energies and $\Delta_{vap}H_{298}$ values, that the E_{coul} for $[C_nC_1Pyrr][Tf_2N]$ is approximately independent of n. Therefore, surface tension is likely to be determined by E_{vdW} and an unknown contribution due to surface orientation. To fully understand the underlying factors that determine macroscopic properties of pyrrolidinium-based ionic liquids will require more extensive studies of their physical properties.

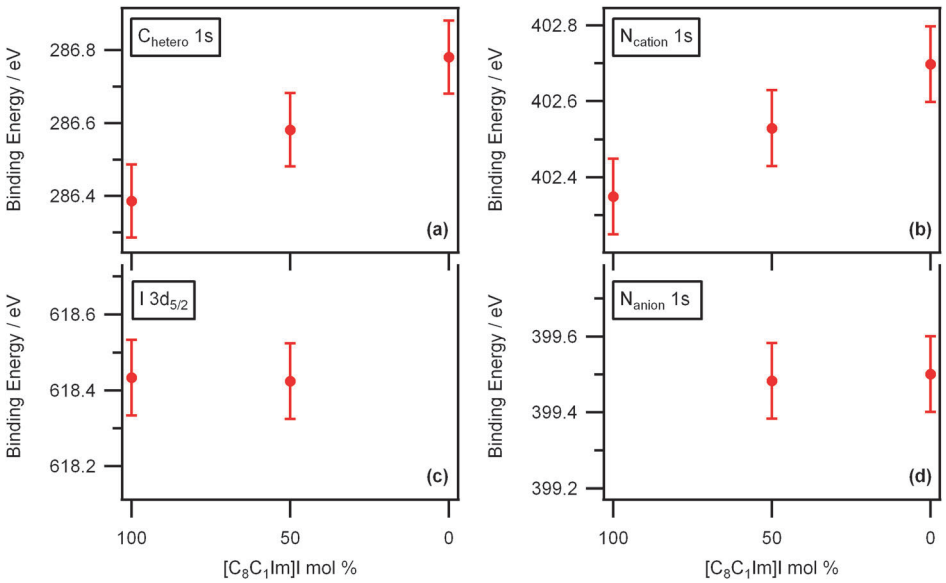

Fig. 7 Binding energy shifts for a 1 : 1 mixture of $[C_8C_1Pyrr][Tf_2N]$: $[C_8C_1Pyrr]I$ and pure ionic liquids $[C_8C_1Pyrr][Tf_2N]$ and $[C_8C_1Pyrr]I$: (a) C_{hetero} 1s, (b) N_{cation} 1s, (c) I $3d_{5/2}$ and (d) N_{anion} 1s. All binding energies were charge corrected by referencing the aliphatic C 1s photoemission peak ($C_{aliphatic}$ 1s) to 285.0 eV. Binding energy shifts for all 10 components are given in Fig. S10.† Please note that the binding energies plotted here are given to two decimal places, whereas those in Table 3 are rounded to one decimal place.

Conclusions

We have successfully measured XP spectra for a range of pyrrolidinium-based ionic liquids, varying both the cation aliphatic chain length, *n*, and the anion. The ionic liquids were demonstrated to be of high purity, allowing conclusions to be drawn on the physicochemical properties of the pyrrolidinium-based ionic liquids. The electronic environments of all elements were identified. A robust fitting model for the C 1s region of pyrrolidinium-based ionic liquids was produced. The binding energy of the aliphatic carbon ($C_{aliphatic}$ 1s) moiety was determined with high confidence. As reliable binding energies were obtained for $C_{aliphatic}$ 1s, charge corrected binding energies (absolute binding energies) for all components could be obtained. Variation of *n*, with the same anion, was shown to have little or no effect on the electronic interaction of the charge-bearing headgroups of the ionic liquid. The binding energy data table presented in this paper may find future use as a standard list of binding energies for pyrrolidinium-based ionic liquids.

Comparisons of the charge corrected binding energies of the pyrrolidinium nitrogen atom, N_{cation} 1s (and also the carbon atoms directly bonded to nitrogen, C_{hetero} 1s) as a function of anion were also carried out. The binding energy for N_{cation} 1s decreased as the basicity of the anion increased, indicating that more charge is transferred from the anion to the cation for more basic anions such as iodide. In particular, mixtures of anions can be used to tune the electronic properties of ionic liquids. Further comparison of the binding energies of the cationic components for imidazolium- and pyrrolidinium-based ionic liquids revealed significant differences. The charge on the nitrogen atom of pyrrolidinium is significantly more electropositive than the nitrogen atoms of imidazolium (when the anion is the same). In addition, the C^2 carbon atom of imidazolium is more electropositive than any of the carbon atoms in pyrrolidinium. This observation agrees with the relative cathodic stability of the cations; pyrrolidinium-based ionic liquids generally have a wider electrochemical window than their imidazolium-based counterparts, due to the relative ease of removal of the C^2 proton from imidazolium.

In general in this study, trends of properties for pyrrolidinium-based ionic liquids have matched those of imidazolium-based ionic liquids. This observation holds for: the effect of *n* on the electronic interaction of the charge-bearing headgroups, and the effect of anions on the electronic environment of the cation for both one anion and two anions, *i.e.*, mixtures. These observations suggest that whilst imidazolium- and pyrrolidinium-based ionic liquids have significantly different properties, the underlying factors that affect these properties are the same for both cations. Initial investigations suggest that these underlying factors can be explained by treating coulombic and van der Waals contributions independently.

Acknowledgements

We would like to thank the EPSRC (EP/D501229/1) for financial support. PL acknowledges the EPSRC for the award of an ARF (EP/D073014/1). The authors are grateful to Ms Emily F. Smith, Drs Alasdair Taylor and Ignacio Villar-Garcia for helpful discussions and critical advice. Mr Andinet Ejigu and Mr Bitu Birru Hurisso are thanked for their help washing some of the ionic liquids prior to investigation by XPS. Dr Peter Gooden and Ms Jo-Anne Corfield are acknowledged for their contributions towards the synthesis of $[C_nC_1Pyrr][Tf_2N]$.

References

1 *Ionic liquids in synthesis*, ed. P. Wasserscheid and T. Welton, Wiley-VCH, Weinheim, 2nd edn, 2008.
2 N. V. Plechkova and K. R. Seddon, *Chem. Soc. Rev.*, 2008, **37**, 123–150.

3 H. Weingärtner, *Angew. Chem., Int. Ed.*, 2008, **47**, 654–670.
4 S. A. Forsyth, S. R. Batten, Q. Dai and D. R. MacFarlane, *Aust. J. Chem.*, 2004, **57**, 121–124.
5 P. Johansson, L. E. Fast, A. Matic, G. B. Appetecchi and S. Passerini, *J. Power Sources*, 2010, **195**, 2074–2076.
6 M. H. Ghatee, M. Zare, A. R. Zolghadr and F. Moosavi, *Fluid Phase Equilib.*, 2010, **291**, 188–194.
7 R. L. Gardas and J. A. P. Coutinho, *Fluid Phase Equilib.*, 2008, **266**, 195–201.
8 T. J. Wooster, K. M. Johanson, K. J. Fraser, D. R. MacFarlane and J. L. Scott, *Green Chem.*, 2006, **8**, 691–696.
9 R. E. Del Sesto, T. M. McCleskey, C. Macomber, K. C. Ott, A. T. Koppisch, G. A. Baker and A. K. Burrell, *Thermochim. Acta*, 2009, **491**, 118–120.
10 V. N. Emel'yanenko, S. P. Verevkin, A. Heintz, J. A. Corfield, A. Deyko, K. R. J. Lovelock, P. Licence and R. G. Jones, *J. Phys. Chem. B*, 2008, **112**, 11734–11742.
11 A. Deyko, K. R. J. Lovelock, J. A. Corfield, A. W. Taylor, P. N. Gooden, I. J. Villar-Garcia, P. Licence, R. G. Jones, V. G. Krasovskiy, E. A. Chernikova and L. M. Kustov, *Phys. Chem. Chem. Phys.*, 2009, **11**, 8544–8555.
12 S. D. Chambreau, G. L. Vaghjiani, A. To, C. Koh, D. Strasser, O. Kostko and S. R. Leone, *J. Phys. Chem. B*, 2010, **114**, 1361–1367.
13 K. R. J. Lovelock, I. J. Villar-Garcia, F. Maier, H. P. Steinrück and P. Licence, *Chem. Rev.*, 2010, **110**, 5158–5190.
14 D. S. Silvester, T. L. Broder, L. Aldous, C. Hardacre, A. Crossley and R. G. Compton, *Analyst*, 2007, **132**, 196–198.
15 M. Shigeyasu, H. Murayama and H. Tanaka, *Chem. Phys. Lett.*, 2008, **463**, 373–377.
16 J. K. Chang, M. T. Lee, W. T. Tsai, M. J. Deng and I. W. Sun, *Chem. Mater.*, 2009, **21**, 2688–2695.
17 J. K. Chang, C. H. Huang, M. T. Lee, W. T. Tsai, M. J. Deng and I. W. Sun, *Electrochim. Acta*, 2009, **54**, 3278–3284.
18 V. Lockett, R. Sedev, S. Harmer, J. Ralston, M. Horne and T. Rodopoulos, *Phys. Chem. Chem. Phys.*, 2010, **12**, 13816–13827.
19 Q. H. Zhang, S. M. Liu, Z. P. Li, J. Li, Z. J. Chen, R. F. Wang, L. J. Lu and Y. Q. Deng, *Chem.–Eur. J.*, 2009, **15**, 765–778.
20 E. F. Smith, I. J. Villar Garcia, D. Briggs and P. Licence, *Chem. Commun.*, 2005, 5633–5635.
21 E. F. Smith, F. J. M. Rutten, I. J. Villar-Garcia, D. Briggs and P. Licence, *Langmuir*, 2006, **22**, 9386–9392.
22 K. R. J. Lovelock, E. F. Smith, A. Deyko, I. J. Villar-Garcia, P. Licence and R. G. Jones, *Chem. Commun.*, 2007, 4866–4868.
23 J. M. Gottfried, F. Maier, J. Rossa, D. Gerhard, P. S. Schulz, P. Wasserscheid and H. P. Steinrück, *Z. Phys. Chem.*, 2006, **220**, 1439–1453.
24 K. R. J. Lovelock, C. Kolbeck, T. Cremer, N. Paape, P. S. Schulz, P. Wasserscheid, F. Maier and H. P. Steinrück, *J. Phys. Chem. B*, 2009, **113**, 2854–2864.
25 H. Hashimoto, A. Ohno, K. Nakajima, M. Suzuki, H. Tsuji and K. Kimura, *Surf. Sci.*, 2010, **604**, 464–469.
26 I. J. Villar-Garcia, E. F. Smith, A. W. Taylor, F. L. Qiu, K. R. J. Lovelock, R. G. Jones and P. Licence, *Phys. Chem. Chem. Phys.*, 2011, **13**, 2797–2808.
27 T. Cremer, C. Kolbeck, K. R. J. Lovelock, N. Paape, R. Wölfel, P. S. Schulz, P. Wasserscheid, H. Weber, J. Thar, B. Kirchner, F. Maier and H. P. Steinrück, *Chem.–Eur. J.*, 2010, **16**, 9018–9033.
28 I. J. Villar-Garcia, K. R. J. Lovelock and P. Licence, 2011, in preparation.
29 N. Papaiconomou, J. Salminen, J. M. Lee and J. M. Prausnitz, *J. Chem. Eng. Data*, 2007, **52**, 833–840.
30 D. R. MacFarlane, P. Meakin, J. Sun, N. Amini and M. Forsyth, *J. Phys. Chem. B*, 1999, **103**, 4164–4170.
31 A. W. Taylor, K. R. J. Lovelock, A. Deyko, P. Licence and R. G. Jones, *Phys. Chem. Chem. Phys.*, 2010, **12**, 1772–1783.
32 C. D. Wagner, L. E. Davis, M. V. Zeller, J. A. Taylor, R. H. Raymond and L. H. Gale, *Surf. Interface Anal.*, 1981, **3**, 211–225.
33 *Surface Analysis by Auger and X-ray Photoelectron Spectroscopy*, ed. D. Briggs and J. T. Grant, IM Publications, Manchester, 2003.
34 C. Kolbeck, T. Cremer, K. R. J. Lovelock, N. Paape, P. S. Schulz, P. Wasserscheid, F. Maier and H. P. Steinrück, *J. Phys. Chem. B*, 2009, **113**, 8682–8688.
35 K. R. J. Lovelock, A. W. Taylor, S. Men, A. Ejigu, D. A. Walsh and P. Licence, 2011, in preparation.
36 K. Shimizu, M. Tariq, M. F. Costa Gomes, L. P. N. Rebelo and J. N. Canongia Lopes, *J. Phys. Chem. B*, 2010, **114**, 5831–5834.
37 R. Wibowo, S. E. W. Jones and R. G. Compton, *J. Chem. Eng. Data*, 2010, **55**, 1374–1376.
38 M. C. Kroon, W. Buijs, C. J. Peters and G. J. Witkamp, *Green Chem.*, 2006, **8**, 241–245.
39 P. Bonhôte, A. P. Dias, N. Papageorgiou, K. Kalyanasundaram and M. Grätzel, *Inorg. Chem.*, 1996, **35**, 1168–1178.
40 J. M. Pringle, J. Golding, K. Baranyai, C. M. Forsyth, G. B. Deacon, J. L. Scott and D. R. MacFarlane, *New J. Chem.*, 2003, **27**, 1504–1510.
41 S. Randstrom, M. Montanino, G. B. Appetecchi, C. Lagergren, A. Moreno and S. Passerini, *Electrochim. Acta*, 2008, **53**, 6397–6401.
42 B. Birru Hurisso, K. R. J. Lovelock and P. Licence, *Phys. Chem. Chem. Phys.*, 2011, submitted.
43 L. Crowhurst, R. Falcone, N. L. Lancaster, V. Llopis-Mestre and T. Welton, *J. Org. Chem.*, 2006, **71**, 8847–8853.
44 J. M. Lee and J. M. Prausnitz, *Chem. Phys. Lett.*, 2010, **492**, 55–59.
45 F. Maier, T. Cremer, C. Kolbeck, K. R. J. Lovelock, N. Paape, P. S. Schulz, P. Wasserscheid and H. P. Steinrück, *Phys. Chem. Chem. Phys.*, 2010, **12**, 1905–1915.
46 H. Jin, B. O'Hare, J. Dong, S. Arzhantsev, G. A. Baker, J. F. Wishart, A. J. Benesi and M. Maroncelli, *J. Phys. Chem. B*, 2008, **112**, 81–92.
47 C. Kolbeck, J. Lehmann, K. R. J. Lovelock, T. Cremer, N. Paape, P. Wasserscheid, A. P. Fröba, F. Maier and H. P. Steinrück, *J. Phys. Chem. B*, 2010, **114**, 17025–17036.
48 M. R. J. Dack, *Chem. Soc. Rev.*, 1975, **4**, 211–229.